JOURNAL OF CATALYSIS **179,** 300–308 (1998)
ARTICLE NO. CA982227

# Oxidative Dehydrogenation of Ethane to Ethene over BaO- and $BaBr_2$-Modified $Ho_2O_3$ Catalysts

C. T. Au,[1] K. D. Chen,[2] H. X. Dai, Y. W. Liu, J. Z. Luo, and C. F. Ng

*Chemistry Department and Center for Surface Analysis and Research, Hong Kong Baptist University, Kowloon Tong, Hong Kong, China*

Received December 29, 1997; revised July 20, 1998; accepted July 21, 1998

**The addition of $BaBr_2$ (<70 mol%) to $Ho_2O_3$ could improve considerably both the $C_2H_6$ conversion and $C_2H_4$ selectivity of the ODE (oxidative dehydrogenation of ethane) reaction. The use of BaO as a modifier was not suitable because the catalyst degraded rapidly due to $BaCO_3$ formation. At 640°C, $C_2H_6:O_2:N_2 = 2:1:4$, and space velocity = 6000 mL $h^{-1}$ $g^{-1}$, $C_2H_6$ conversion of 70.6%, $C_2H_4$ selectivity of 80.2%, and $C_2H_4$ yield of 56.6% were observed over the 50 mol% $BaBr_2/Ho_2O_3$ catalyst after a reaction time of 1 h. We conclude that the addition of $BaBr_2$ to $Ho_2O_3$ can (i) enhance oxygen activation, (ii) protect a certain amount of active basic sites from $CO_2$ poisoning, and (iii) suppress $C_2H_4$ deep oxidation. It is possible that the presence of $Br^-$ ions could have induced the formation of new active sites suitable for $C_2H_4$ generation. However, we observed continuous leaching of bromine during the ODE reaction, and the 50 mol% $BaBr_2/Ho_2O_3$ catalyst gradually degenerated to a somewhat aged $BaO/Ho_2O_3$ catalyst. After 40 h of reaction, the $C_2H_6$ conversion, $C_2H_4$ selectivity, and $C_2H_4$ yield diminished to 51.8, 63.8, and 33.0%, respectively.** 

## INTRODUCTION

The oxidative dehydrogenation of ethane (ODE) to ethene is a very important chemical process as ethene is the starting material for the production of valuable chemicals such as styrene, ethylbenzene, ethanol, acetaldehyde, vinyl acetate, etc. In the past years, many researchers have studied the ODE reaction over catalysts such as Li/MgO (1, 2), $Re_2O_3$ (rare earth oxides) (3, 4), *M*-Mo/$SiO_2$ (*M* = Li, Na, K, Rb, Cs) (5), *M*-V/$SiO_2$ (*M* = Li, Na, K, Rb, Cs) (6), Na/$CeO_2$ (7), $La_{1-x}Sr_xFeO_{3-\delta}$ (8), *M*-ZSM-5 (*M* = Nb, V, Co, Cu) (9), SmOF (10). Among the catalysts studied, perhaps the most effective ones were the "Li/MgO" catalysts reported by Lunsford's group in numerous publications. To cite one as an example (1), with the reaction conditions of 620°C, $C_2H_6:O_2:He = 290:290:180$ (torr), gas flow rate = 60 mL $min^{-1}$, total pressure = 760 torr, and 5 g catalyst, they obtained 75% ethane conversion and 77% ethene selectivity (i.e. 58% ethene yield) over a $Li^+$-MgO-$Cl^-$ catalyst with a ratio of Cl/Li $\geq$ 0.9 after 50 h on stream. Later, they found that the addition of a certain amount of lanthanide oxides (e.g., $Dy_2O_3$) to the catalyst could lower the reaction temperature to 570°C with the performance almost unchanged (11).

Being one of the secondary reactions of the oxidative coupling of methane (OCM), the ODE process has been studied along with the OCM reaction by many researchers (e.g. (2, 4, 7, 12, 13)). It has been found that some OCM catalysts with high $C_2H_4/C_2H_6$ ratio are also good ODE catalysts (2). In the studies of the OCM reaction, several groups have achieved large ethene-to-ethane ratio by introducing chlorine into the catalyst or by passing a chlorine-containing compound over the catalyst during the reaction (14–18). Based on these results, many chlorine-containing catalysts were studied for the ODE reaction with the promotion effects of chlorine being cited. As suggested by Lunsford *et al.* (2), the presence of $Cl^-$ ions in the catalyst might improve the catalytic activity by preventing the active sites from $CO_2$ poisoning; the $Cl^-$ ions could also lower the reactivity of oxygen species so that they were capable of activating the weaker C-H bond in ethane (98 kcal $mol^{-1}$), but were less effective in activating the stronger C-H bond in ethene (>108 kcal $mol^{-1}$). In our laboratory, we have studied the OCM performances of a number of La-Ba-*X* (19–22), Y-Ba-*X* (23, 24), and Ho-Ba-*X* (*X* = F, Cl, Br) (25) catalysts; the results indicated that the addition of halides, especially bromine, on some rare earth oxide catalysts could significantly enlarge the ethene-to-ethane ratio. For example, the $C_2H_4/C_2H_6$ ratio in OCM reaction at 750°C was augmented from 1.4 to 10.6 when 50 mol% of $BaBr_2$ was added to $Ho_2O_3$ (25). We envisaged that the catalysts with high ethene-to-ethane ratio in the OCM reaction might also be good catalysts for the ODE reaction. In this paper, we report the promotion effects of $BaBr_2$ on $Ho_2O_3$ in this aspect.

## EXPERIMENTAL

The $BaBr_2/Ho_2O_3$, 50 mol% *M*O/$Ho_2O_3$ (*M* = Mg, Ca, Sr, and Ba), and 50 mol% $BaCO_3/Ho_2O_3$ catalysts were

[1] To whom correspondence should be addressed. E-mail: pctau@hkbu.edu.hk.

[2] Present address: Department of Chemical Engineering, UC Berkeley, CA 94720.



0021-9517/98 $25.00

prepared by wet-impregnation of $Ho_2O_3$ powder, respectively, with aqueous solution of $BaBr_2$, $M(NO_3)_2$ ($M$ = Mg, Ca, Sr, and Ba), and $BaCO_3$ followed by evaporation. The pastes were dried at 120°C overnight and calcined at 800°C for 5 h before being ground, tableted, crushed, and sieved into 40–80 mesh.

The ODE reactions were carried out with 0.5 g of the catalyst in a fixed-bed quartz flow micro-reactor (ID = 4 mm) at atmospheric pressure. The reaction temperatures ranged from 500 to 660°C at 20°C intervals. A mixture of ethane and air was passed through the micro-reactor. The flow-rate was regulated by a mass flow controller and was 14.8 mL $min^{-1}$ for ethane, and 35.2 mL $min^{-1}$ for air; giving a space velocity of 6000 mL $h^{-1}$ $g^{-1}$ and a $C_2H_6/O_2$ molar ratio of 2/1. For the studies of $C_2H_4$ oxidation, a mixture of $C_2H_4$ and air was used, instead, to make up a $C_2H_4/O_2$ molar ratio of 2/1. The product distribution was determined by a Shimadzu 8A TCD gas chromatograph with Porapark Q and 5A molecular sieve columns.

For the studies of effects of space velocity on the performances of the catalysts, the reactant gas ($C_2H_6/O_2$ molar ratio, 2/1) was carried into the micro-reactor in pulses (pulse size, 65.7 $\mu$L) by helium at space velocities ranging from 1500 to 6000 mL $h^{-1}$ $g^{-1}$. The product distribution was determined on line by a HP G1800A mass spectrometer.

The phase compositions of the catalysts were determined by X-ray diffraction (XRD, D-MAX, Rigaku), whereas X-ray photoelectron spectroscopy (XPS, Leybold Heraeus-Shengyang SKL-12) was used to characterize the surface. The specific surface areas of the catalysts were measured and calculated according to the BET method. The continuous flow chromatographic technique was adopted with helium as the carrier gas and nitrogen as the adsorbate.

For the $O_2$- and $CO_2$-TPD studies, the samples (0.2 g) were placed in the middle of a quartz micro-reactor with 4-mm ID. The outlet gases were analyzed on line by mass spectrometry (HP G1800A). The heating rate was 15°C $min^{-1}$ and the temperature range was from room temperature to 800°C. Before performing the $O_2$- TPD experiments, the samples were first calcined *in situ* at 800°C for 30 min under an oxygen flow of 15 mL $min^{-1}$ followed by cooling in oxygen to room temperature and then purging with helium (flow rate, 20 mL $min^{-1}$) for 30 min. Before the $CO_2$- TPD experiments, the catalysts were first calcined *in situ* at 800°C for 20 min under an oxygen flow of 15 mL $min^{-1}$, followed by purging with helium (20 mL $min^{-1}$) for 30 min and cooling in helium to room temperature, before exposure to a flow of $CO_2$ gas (20 mL $min^{-1}$) for 10 min at room temperature and helium purging afterward for 20 min.

The measurement of the amount of reducible oxygen was also performed on the MS (HP G1800A) system. The catalyst (0.2 g) was placed in a quartz reactor and was first reduced in $H_2$ at 800°C for 1 h, followed by helium purging (flow rate, 20 mL $min^{-1}$) for 10 min and then $O_2$-pulsing at the same temperature. The pulse size of $O_2$ was 65.7 $\mu$L (at 25°C, 1 atm). We kept on pulsing $O_2$ over the reduced sample until, after passing the catalyst, there was no observable decrease in the $O_2$ pulse size. The total amount of $O_2$ absorbed by the catalyst was then calculated and expressed in moles per gram of catalyst.

Temperature-programmed reduction (TPR) was conducted by using a 7% $H_2$–93% $N_2$ (v/v) mixture. The flow rate of the carrier gas was 50 mL $min^{-1}$ and a thermal conductivity detector was used. The amount of sample used was 0.2 g and the heating rate was 10°C $min^{-1}$. Before performing the TPR experiments, the sample was first calcined *in situ* at 800°C for 30 min under an oxygen flow of 15 mL $min^{-1}$, followed by cooling in oxygen to room temperature.

For the analysis of bromine content, the catalyst was first digested in 0.1 *M* NaOH solution. The resulting solution was neutralized by 2 *M* $HNO_3$ solution and titrated against standardized $AgNO_3$ solution using 0.005 *M* potassium chromate as indicator.

## RESULTS

### *Catalytic Performance*

Table 1 shows the ODE performances of $Ho_2O_3$, 50 mol% $MO/Ho_2O_3$ ($M$ = Mg, Ca, Sr, and Ba), and 50 mol% $BaCO_3/Ho_2O_3$ catalysts at 640°C. For pure $Ho_2O_3$, oxygen conversion was 84.7%, ethane conversion was 43.4%, and $C_2H_4$ selectivity was 51.4%, giving a $C_2H_4$ yield of 22.3%. The use of $MO$ ($M$ = Mg, Ca, Sr, and Ba) as modifiers showed negative effects. For the four 50 mol% $MO/Ho_2O_3$ catalysts, $C_2H_6$ conversions and $C_2H_4$ selectivities were lower than those of the undoped $Ho_2O_3$, but the oxygen conversions were higher (>98%). $C_2H_4$ yield was 13.4% over the 50 mol% $MgO/Ho_2O_3$ catalyst and was ca 21% over the other three $MO/Ho_2O_3$ catalysts. We found

**TABLE 1**

**ODE Performances after an On-Stream Time of 1 h over $Ho_2O_3$, 50 mol% $MO/Ho_2O_3$ ($M$ = Mg, Ca, Sr, and Ba) and 50 mol% $BaCO_3/Ho_2O_3$ at 640°C**

| Catalyst | Conversion (%) | | Selectivity (%) | | | Yield (%) | Rate of $C_2H_6$ reaction ($10^{18}$ molecules $m^{-2}$ $s^{-1}$) |
|---|---|---|---|---|---|---|---|
| | $C_2H_6$ | $O_2$ | $CO_x$ | $CH_4$ | $C_2H_4$ | $C_2H_4$ | |
| Blank[a] | 5.0 | — | 12.0 | 0 | 88.0 | 4.4 | — |
| $Ho_2O_3$ | 43.4 | 84.7 | 46.8 | 1.8 | 51.4 | 22.3 | 4.43 |
| $MgO/Ho_2O_3$ | 33.7 | 99.4 | 58.7 | 1.6 | 39.7 | 13.4 | 3.72 |
| $CaO/Ho_2O_3$ | 40.9 | 98.8 | 47.6 | 2.2 | 50.2 | 20.6 | 4.52 |
| $SrO/Ho_2O_3$ | 42.2 | 98.5 | 48.8 | 2.6 | 48.5 | 20.5 | 4.66 |
| $BaO/Ho_2O_3$ | 41.2 | 98.7 | 46.4 | 2.8 | 50.8 | 20.9 | 4.97 |
| $BaCO_3/Ho_2O_3$ | 40.8 | 98.8 | 46.7 | 2.9 | 50.4 | 20.6 | — |

[a] Tested at 660°C.

**TABLE 2**

**ODE Performances after an On-Stream Time of 1 h over 50 mol% $BaX_2/Ho_2O_3$ ($X$ = F, Cl, and Br) at 640°C**

| Catalyst | Conversion (%) | | Selectivity (%) | | | Yield (%) | Rate of $C_2H_6$ reaction ($10^{18}$ molecules $m^{-2}$ $s^{-1}$) |
|---|---|---|---|---|---|---|---|
| | $C_2H_6$ | $O_2$ | $CO_x$ | $CH_4$ | $C_2H_4$ | $C_2H_4$ | |
| BFH | 47.1 | 98.6 | 34.9 | 2.0 | 63.2 | 29.8 | 5.20 |
| BCH | 55.9 | 96.4 | 30.1 | 2.0 | 67.8 | 37.9 | 6.18 |
| BBH | 70.6 | 93.9 | 17.4 | 2.4 | 80.2 | 56.6 | 7.80 |

*Note.* BFH: $BaF_2/Ho_2O_3$; BCH: $BaCl_2/Ho_2O_3$; BBH: $BaBr_2/Ho_2O_3$.

**TABLE 4**

**Results of the Oxidation of Ethane and Ethene after an On-Stream Time of 1 h over $Ho_2O_3$, 50 mol% $BaO/Ho_2O_3$, and 50 mol% $BaBr_2/Ho_2O_3$ Catalysts at 640°C**

| Catalyst | Oxidation of $C_2H_4$ | Oxidation of $C_2H_6$ | |
|---|---|---|---|
| | $C_2H_4$ conv. (%) | $C_2H_6$ conv. (%) | $C_2H_4$ sel. (%) |
| $Ho_2O_3$ | 29.2 | 43.4 | 51.4 |
| 50 mol% $BaO/Ho_2O_3$ | 31.8 | 41.2 | 50.8 |
| 10 mol% $BaBr_2/Ho_2O_3$ | 26.0 | 54.8 | 65.8 |
| 50 mol% $BaBr_2/Ho_2O_3$ | 17.5 | 70.6 | 80.2 |

that after an on-stream time of 1 h, a 50 mol% $BaO/Ho_2O_3$ catalyst behaved exactly as a 50 mol% $BaCO_3/Ho_2O_3$ catalyst.

The performances of the 50 mol% $BaX_2/Ho_2O_3$ ($X$ = F, Cl, and Br) catalysts after 1 h of ODE reactions at 640°C are shown in Table 2. It could be observed that the performances of the $BaX_2$-promoted samples were better than that of pure $Ho_2O_3$. For the three 50 mol% $BaX_2/Ho_2O_3$ catalysts, the $C_2H_6$ conversion and $C_2H_4$ selectivity followed the sequence of 50 mol% $BaBr_2/Ho_2O_3$ > 50 mol% $BaCl_2/Ho_2O_3$ > 50 mol% $BaF_2/Ho_2O_3$. For the 50 mol% $BaBr_2/Ho_2O_3$ catalyst, oxygen conversion was 93.9%, ethane conversion was 70.6%, and $C_2H_4$ selectivity was 80.2%, giving a $C_2H_4$ yield of 56.6%. A 90 mol% $BaBr_2/Ho_2O_3$ catalyst performed rather poorly; the $O_2$ and $C_2H_6$ conversions were, respectively, ca 64 and 41%, and the $C_2H_4$ selectivity was ca 90%, giving a $C_2H_4$ yield of ca 37%.

Table 3 shows the catalytic performances of the pure $Ho_2O_3$, 50 mol% $BaO/Ho_2O_3$, and 50 mol% $BaBr_2/Ho_2O_3$ samples when pulses of $C_2H_6/O_2$ were carried to the catalysts at 640°C by helium flows with space velocities ranging from 1500 to 6000 mL $h^{-1}$ $g^{-1}$. The experiments were designed in such a way that the occurrences of hot spots and Br leaching during the time of evaluation were minimized. One can see that over the three catalysts, both $O_2$ and $C_2H_6$ conversions decreased while the $C_2H_4$ selectivity increased with the increase in space velocity. The data in Table 3 also illustrate that at space velocities equal to or higher than 3000 mL $h^{-1}$ $g^{-1}$, where $O_2$ conversions were less than 80%, the 50 mol% $BaBr_2/Ho_2O_3$ catalyst was superior to the other two catalysts in $C_2H_4$ selectivity and yield. In other words, the good yield of $C_2H_4$ over the $BaBr_2$-promoted catalyst is attributable to real catalysis and real chemistry of the catalyst.

**TABLE 3**

**The Catalytic Performances of the Undoped $Ho_2O_3$, 50 mol% $BaO/Ho_2O_3$, and 50 mol% $BaBr_2/Ho_2O_3$ Catalysts as Related to the Space Velocity of a $C_2H_6/O_2$ Pulse at 640°C**

| Catalyst | Space velocity (mL $h^{-1}$ $g^{-1}$) | Conversion (%) | | Selectivity (%) | | | Yield (%) |
|---|---|---|---|---|---|---|---|
| | | $C_2H_6$ | $O_2$ | $CO_x$ | $CH_4$ | $C_2H_4$ | $C_2H_4$ |
| $Ho_2O_3$ | 1,500 | 68.9 | 86.2 | 67.1 | 0.4 | 32.5 | 22.4 |
| | 3,000 | 66.6 | 65.4 | 62.4 | 0.8 | 36.8 | 24.5 |
| | 4,500 | 63.8 | 55.6 | 62.2 | 0.9 | 36.9 | 23.5 |
| | 6,000 | 63.4 | 50.1 | 60.2 | 1.0 | 38.8 | 24.6 |
| $BaO/Ho_2O_3$ | 1,500 | 70.1 | 90.5 | 64.8 | 0.6 | 34.6 | 24.3 |
| | 3,000 | 68.3 | 70.0 | 59.3 | 0.8 | 39.9 | 27.3 |
| | 4,500 | 65.8 | 59.9 | 58.0 | 0.9 | 41.1 | 27.0 |
| | 6,000 | 65.4 | 58.8 | 56.5 | 1.0 | 42.5 | 27.8 |
| $BaBr_2/Ho_2O_3$ | 1,500 | 73.1 | 99.9 | 42.9 | 0.4 | 56.7 | 41.4 |
| | 3,000 | 71.5 | 77.7 | 39.0 | 0.8 | 60.2 | 43.0 |
| | 4,500 | 65.9 | 56.1 | 38.6 | 0.8 | 60.6 | 39.9 |
| | 6,000 | 65.5 | 50.9 | 38.2 | 0.9 | 60.9 | 39.9 |

The results of the oxidation of ethene and ethane over various catalysts are listed in Table 4. It is apparent that the addition of $BaBr_2$ to $Ho_2O_3$ would inhibit significantly the oxidation of $C_2H_4$, but enhance both the conversion of $C_2H_6$ and selectivity of $C_2H_4$ in the ODE reaction. For the four catalysts tested, $C_2H_4$ conversion in $C_2H_4$ oxidation followed the sequence of 50 mol% $BaBr_2/Ho_2O_3$ < 10 mol% $BaBr_2/Ho_2O_3$ < $Ho_2O_3$ < 50 mol% $BaO/Ho_2O_3$, whereas $C_2H_4$ selectivity and $C_2H_6$ conversion in $C_2H_6$ oxidation over the catalysts showed the reverse order.

Figure 1 shows the catalytic performance of the 50 mol% $BaBr_2/Ho_2O_3$ catalyst at 640°C as related to reaction time. One can see that the values of $C_2H_6$ conversion, $C_2H_4$ selectivity, and $C_2H_4$ yield decreased gradually within the first 35 h, and then stayed nearly unchanged in the last 5 h, with $C_2H_6$ conversion, $C_2H_4$ selectivity, and $C_2H_4$ yield equal to 51.8, 63.8, and 33.0%, respectively. The performance of a 50 mol% $BaO/Ho_2O_3$ catalyst was rather stable from an on-stream time of 1 to 40 h; the $C_2H_6$ conversion, $C_2H_4$ selectivity, and $C_2H_4$ yield stayed at ca 41, 51, and 21%, respectively.

### *XRD, BET, XPS, and Bromine Content Studies*

XRD results of the 50 mol% $BaO/Ho_2O_3$ and 50 mol% $BaBr_2/Ho_2O_3$ catalysts are shown in Table 5. For the fresh

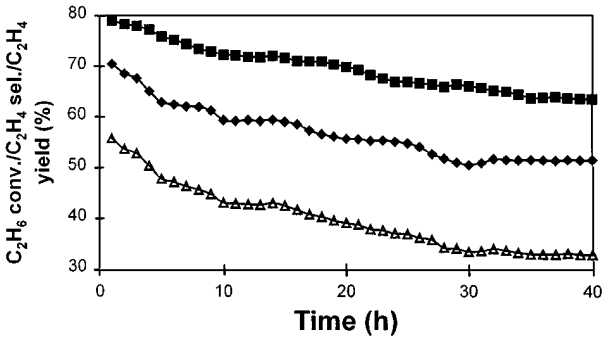


**FIG. 1.** The catalytic performance of 50 mol% $BaBr_2/Ho_2O_3$ as related to reaction time: (■) $C_2H_4$ selectivity; (◆) $C_2H_6$ conversion; (△) $C_2H_4$ yield.

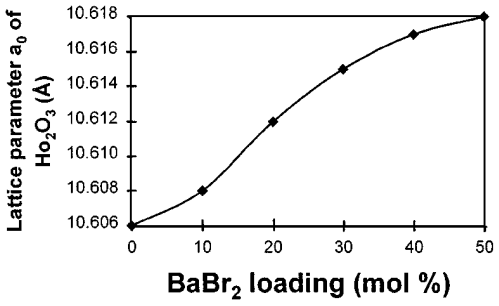


**FIG. 2.** The change of the lattice parameter, $a_0$, of $Ho_2O_3$ in $BaBr_2/Ho_2O_3$ catalysts as related to $BaBr_2$ loading.

50 mol% $BaBr_2/Ho_2O_3$ catalyst, no new phases such as barium and holmium oxybromides were observed besides the monoclinic $BaBr_2 \cdot 2H_2O$ and cubic $Ho_2O_3$ phases. After 40 h of ODE reaction, lines due to $BaCO_3$ were observed. For the fresh 50 mol% $BaO/Ho_2O_3$ catalyst, there were the phases of BaO, $BaCO_3$, and $Ho_2O_3$. After the ODE reaction, the BaO phase disappeared due to the conversion of BaO to $BaCO_3$.

Based on the *d* values of XRD peaks, the $Ho_2O_3$ lattice parameters, $a_0$, of various samples were calculated. It was found that the lattice parameter of $Ho_2O_3$ in the $BaBr_2$- or BaO-doped samples was larger than that of the undoped $Ho_2O_3$. Figure 2 shows the changes of $a_0$ in the $BaBr_2/Ho_2O_3$ catalysts. It can be seen that with the increase of $BaBr_2$ loading, $a_0$ increased too. The length ($a_0$) of the cubic unit cell edge of $Ho_2O_3$ is 10.606 Å. For the 50 mol% $BaBr_2/Ho_2O_3$ and 50 mol% $BaO/Ho_2O_3$ catalysts, $a_0$ values were 10.618 and 10.612 Å, respectively. Compared to the fresh ones, the samples measured after 40 h of ODE reactions showed little changes in $a_0$ values.

BET surface areas of the $Ho_2O_3$, 50 mol% $BaO/Ho_2O_3$, and 50 mol% $BaBr_2/Ho_2O_3$ samples were measured. The specific surface area of pure $Ho_2O_3$ was 1.3 $m^2\,g^{-1}$. The specific surface areas of the 50 mol% $BaO/Ho_2O_3$ and 50 mol% $BaBr_2/Ho_2O_3$ catalysts were 1.1 and 1.2 $m^2\,g^{-1}$, respectively; a little bit smaller than that of pure $Ho_2O_3$. There were little changes in specific surface area of the samples during the ODE reaction as indicated by the BET measurements performed after the ODE reaction.

Based on the XPS peak areas and the atomic sensitivity factors of the elements, the surface bromine compositions of a 50 mol% $BaBr_2/Ho_2O_3$ catalyst before and after ODE reactions of 4 h, 20 h, and 40 h were calculated and are shown in Table 6. One can see that the surface bromine composition decreased continuously with reaction time. After 40 h, the surface bromine composition decreased by ca 75% as compared to the fresh sample.

The results of bromine content analysis of a 50 mol% $BaBr_2/Ho_2O_3$ catalyst before and after ODE reactions of 4 h, 20 h, and 40 h are also shown in Table 6. It can be observed that the bromine composition of the catalyst also decreased continuously during the reaction. After 40 h, the total bromine loss was ca 34% of the original content. A 50 mol% $BaBr_2/Ho_2O_3$ catalyst at 640°C in a flow of $O_2$ (20 mL $min^{-1}$) for 40 h did not show any loss of Br. Hence, the leaching of Br was not a result of thermal instability of the catalyst.

### *TPR, $O_2$-TPD, and $O_2$-Pulse Studies*

TPR profiles of the $Ho_2O_3$, 50 mol% $BaO/Ho_2O_3$, and 50 mol% $BaBr_2/Ho_2O_3$ samples are shown in Fig. 3. There were two weak reduction peaks at ca 690 and 770°C in the TPR profile of pure $Ho_2O_3$. For the 50 mol% $BaBr_2/Ho_2O_3$ sample there were no significant changes in peak position

**TABLE 5**

**XRD Results of 50 mol% $BaO/Ho_2O_3$ and 50 mol% $BaBr_2/Ho_2O_3$ Catalysts before and after ODE Reaction**

| Catalysts | Crystal structure present | |
|---|---|---|
| | Before reaction | After reaction |
| $Ho_2O_3$ | $Ho_2O_3$ (s) | $Ho_2O_3$ (s) |
| 50 mol% $BaO/Ho_2O_3$ | $Ho_2O_3$ (s), BaO (m), $BaCO_3$ (w) | $Ho_2O_3$ (s), $BaCO_3$ (m) |
| 50 mol% $BaBr_2/Ho_2O_3$ | $Ho_2O_3$ (s), $BaBr_2 \cdot 2H_2O$ (m) | $Ho_2O_3$ (s), $BaCO_3$ (w), $BaBr_2 \cdot 2H_2O$ (m) |

*Note.* $Ho_2O_3$ is cubic. BaO is tetragonal. $BaCO_3$ is orthorhombic. $BaBr_2 \cdot 2H_2O$ is monoclinic. s, strong; m, medium; w, weak.

**TABLE 6**

**Br Content on the Surface and in the Bulk of 50 mol% $BaBr_2/Ho_2O_3$ Catalyst before (BR) and after ODE Reaction of 4 h (AR4), 20 h (AR20), and 40 h (AR40)**

| | BR | AR4 | AR20 | AR40 |
|---|---|---|---|---|
| Surface Br content (mol%) | 8.0 | 5.6 | 2.9 | 2.0 |
| Bulk Br content (wt%) | 22.1 | 19.4 | 16.2 | 14.6 |

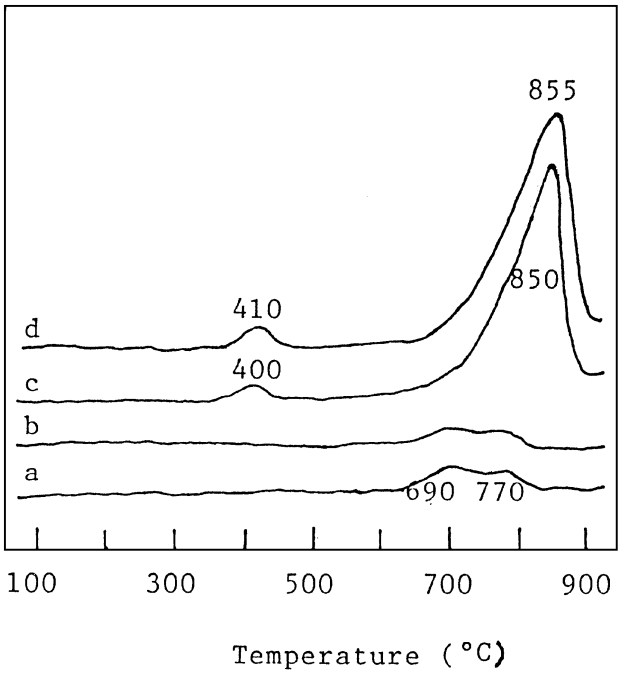


**FIG. 3.** TPR profiles of (a) $Ho_2O_3$, (b) 50 mol% $BaBr_2/Ho_2O_3$, (c) 50 mol% $BaO/Ho_2O_3$ catalysts, and (d) a 50 mol% $BaO/Ho_2O_3$ catalyst with $H_2$ pretreatment at 850°C.

and peak shape, compared to that of $Ho_2O_3$. There was a slight decrease in the peak area, indicating that there was a lesser amount of reducible oxygen in the sample. For the 50 mol% $BaO/Ho_2O_3$ catalyst, a weak reduction peak was detected at ca 400°C and a strong one was observed at ca 850°C. Pretreating the 50 mol% $BaO/Ho_2O_3$ catalyst in a flow of $H_2$ (20 mL $min^{-1}$) for 1 h at 850°C before $O_2$ calcining would give a TPR spectrum of similar profile. Since carbonates that were unstable at or below 850°C would have already been removed in $H_2$-pretreatment, the reduction peak at 850°C was genuinely due to the removal of oxygen from the catalyst.

In order to estimate the amount of reducible oxygen existing in the $Ho_2O_3$, 50 mol% $BaO/Ho_2O_3$, and $BaBr_2/Ho_2O_3$ catalysts, the samples were first reduced in $H_2$ at 800°C and then pulses of $O_2$ were passed through the catalysts at the same temperature. From the amount of $O_2$ absorbed, one could estimate indirectly the amount of oxygen removed in $H_2$-reduction. The idea was based on the assumption that the vacancies generated in $H_2$-reduction would be occupied eventually by oxygen ions during $O_2$ pulsing. Table 7 shows the amount of $O_2$ absorbed at 800°C before the occurrence of zero diminution in $O_2$ pulse size over the catalysts. It is clear that the amount of reducible oxygen in the 50 mol% $BaO/Ho_2O_3$ sample was much larger than that in the undoped $Ho_2O_3$. The amount of oxygen atoms removed from the fresh 50 mol% $BaO/Ho_2O_3$ sample during $H_2$ treatment at 800°C was $25.6 \times 10^{-6}$ mol $g^{-1}$.

**TABLE 7**

**The Amount of Oxygen Absorbed at 800°C over the $H_2$-reduced (800°C) $Ho_2O_3$, $BaBr_2/Ho_2O_3$, and 50 mol% $BaO/Ho_2O_3$ Catalysts**

| Catalyst | $Ho_2O_3$ | BOH | BBH10 | BBH50 | BBH90 |
|---|---|---|---|---|---|
| $O_2$ absorption ($10^{-6}$ mol $g^{-1}$) | 5.2 | 12.8 | 5.1 | 3.0 | 0.7 |

*Note.* BOH: 50 mol% $BaO/Ho_2O_3$; BBH10: 10 mol% $BaBr_2/Ho_2O_3$; BBH50: 50 mol% $BaBr_2/Ho_2O_3$; BBH90: 90 mol% $BaBr_2/Ho_2O_3$.

We proposed that the removal of oxygen could be from the surface as well as from the bulk and the catalyst could function in a redox fashion. For the $BaBr_2/Ho_2O_3$ catalysts, the amount of reducible oxygen decreased with the increase in $BaBr_2$ composition, suggesting that with the increase in $BaBr_2$ composition the amount of oxygen that could be reduced in the $BaBr_2/Ho_2O_3$ catalysts decreased.

The $O_2$-TPD profiles of pure $Ho_2O_3$, 50 mol% $BaO/Ho_2O_3$, and $BaBr_2/Ho_2O_3$ catalysts with different $BaBr_2$ compositions are shown in Fig. 4. For pure $Ho_2O_3$, there was only one $O_2$ desorption peak at ca 430°C in the $O_2$-TPD profile. With the addition of $BaBr_2$ to $Ho_2O_3$, the desorption peak at 430°C decreased in area and shifted to ca 480°C (Figs. 4a–d). For the 50 mol% $BaO/Ho_2O_3$ catalyst

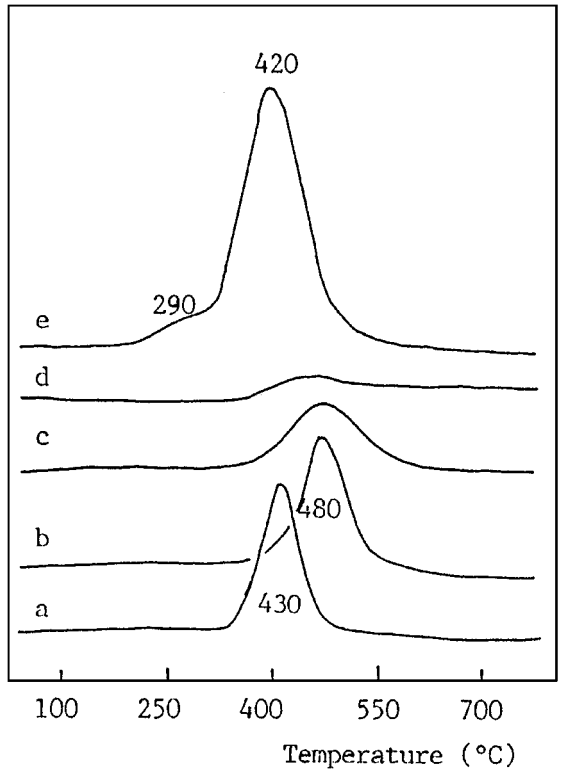


**FIG. 4.** $O_2$-TPD profiles of (a) $Ho_2O_3$, (b) 10 mol% $BaBr_2/Ho_2O_3$, (c) 50 mol% $BaBr_2/Ho_2O_3$, (d) 90 mol% $BaBr_2/Ho_2O_3$, and (e) 50 mol% $BaO/Ho_2O_3$ catalysts.

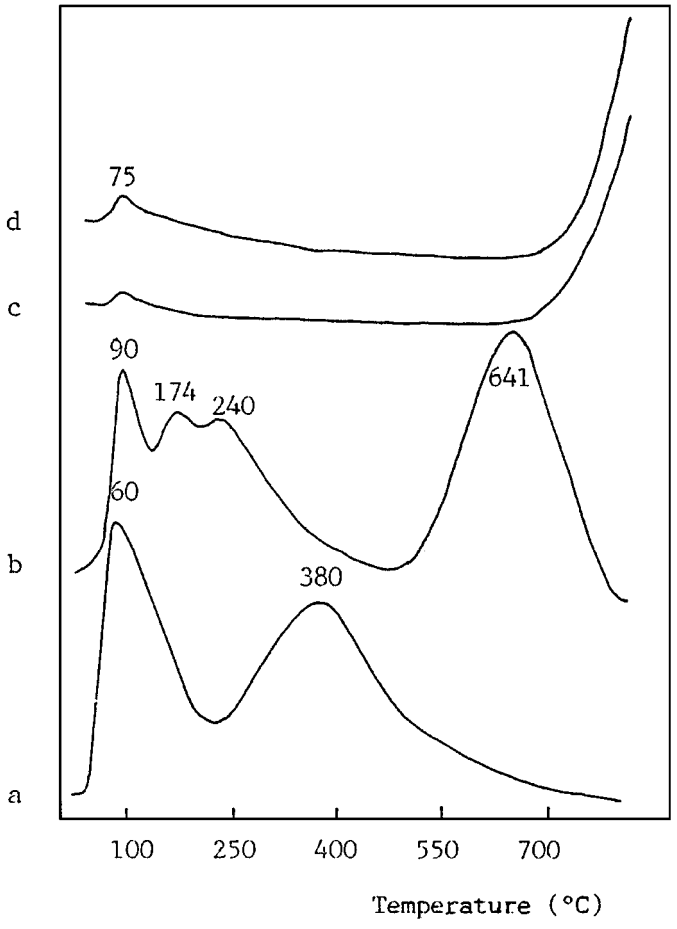


**FIG. 5.** $CO_2$-TPD profiles of (a) fresh $Ho_2O_3$, (b) fresh 50 mol% $BaBr_2/Ho_2O_3$, (c) 50 mol% $BaBr_2/Ho_2O_3$ after ODE reaction of 40 h, and (d) 50 mol% $BaO/Ho_2O_3$ catalysts.

(Fig. 4e), a strong $O_2$ desorption peak at ca 420°C with a shoulder at ca 290°C was observed, and the total peak area was much bigger than that of the undoped $Ho_2O_3$.

### *$CO_2$-TPD Results*

Figure 5 shows the $CO_2$-TPD profiles of undoped $Ho_2O_3$, 50 mol% $BaO/Ho_2O_3$, and 50 mol% $BaBr_2/Ho_2O_3$. Two desorption peaks at ca 60 and 380°C were detected in the $CO_2$-TPD profile of undoped $Ho_2O_3$. For the 50 mol% $BaO/Ho_2O_3$ catalyst, only a very small desorption peak was observed at ca 75°C and large desorption of $CO_2$ was observed above 750°C (Fig. 5d). In the temperature range of 120 to 700°C, there was no $CO_2$ desorption. The $CO_2$-TPD profile of the fresh 50 mol% $BaBr_2/Ho_2O_3$ sample was different from that of $Ho_2O_3$ or $BaO/Ho_2O_3$. Four desorption peaks at ca 90, 174, 240, and 641°C were observed, and the desorption peak at ca 641°C was the largest in area (Fig. 5b). After 40 h of ODE reaction, the $CO_2$-TPD profile of the 50 mol% $BaBr_2/Ho_2O_3$ catalyst became very similar to that of a 50 mol% $BaO/Ho_2O_3$ catalyst (Fig. 5c).

## DISCUSSION

### *Modification of $Ho_2O_3$ by MO ($M$ = Mg, Ca, Sr, and Ba) and $BaX_2$ ($X$ = F, Cl, and Br)*

Based on the results of catalytic performance, one can see that the undoped $Ho_2O_3$ catalyst showed moderate catalytic activity and $C_2H_4$ selectivity (Table 1). The use of $MO$ ($M$ = Mg, Ca, Sr, and Ba) as modifiers exhibited negative effects on $Ho_2O_3$ (Table 1). We conclude that during the ODE reaction, the $MO/Ho_2O_3$ catalysts degraded rather rapidly to $MCO_3/Ho_2O_3$. Taking the $BaO/Ho_2O_3$ catalyst as an example, the results in Table 3 show that it was superior to $Ho_2O_3$ in catalytic performance initially. The pulse experiment was conducted with the ageing of the catalyst minimized and the data in Table 3 should represent a "real" 50 mol% $BaO/Ho_2O_3$ catalyst. The results in Table 1, however, are the activities after an on-stream time of 1 h and the data imply that the ageing of the catalyst was rather rapid and a degraded 50 mol% $BaO/Ho_2O_3$ catalyst was inferior to $Ho_2O_3$. As indicated by the XRD results in Table 5, the BaO in the $BaO/Ho_2O_3$ catalyst changed completely to $BaCO_3$ during ODE reactions. We believe that similar reaction of carbonate formation happened on the $MgO/Ho_2O_3$, $CaO/Ho_2O_3$, and $SrO/Ho_2O_3$ catalysts. The consequence was the degradation of the catalysts.

The addition of $BaX_2$ ($X$ = F, Cl, and Br) to $Ho_2O_3$ could improve the catalytic performance significantly (Table 2). Among the three 50 mol% $BaX_2/Ho_2O_3$ catalysts, the $BaBr_2$-promoted one showed the highest $C_2H_6$ conversion and $C_2H_4$ selectivity (Table 2). As shown in Fig. 1, the catalytic activity and $C_2H_4$ selectivity of the 50 mol% $BaBr_2/Ho_2O_3$ catalyst decreased with reaction time. The drop in $C_2H_6$ conversion was not due to surface area variation since the BET surface area of the sample did not change during the 40 h of reaction. Based on the analytical results of bromine contents on the surface as well as in the bulk of the catalyst, we know that there was continuous bromine leaching. It is likely that the relatively high reactivity in the first 35 h was due to Br liberated from the catalyst. A gas phase reaction involving bromine radicals with the catalyst serving as "initiator" is a possible reaction mechanism. XRD investigation (Table 5) showed that $BaCO_3$ was formed during the ODE reaction. The $CO_2$-TPD profile of the used sample was rather similar to that of an aged $BaO/Ho_2O_3$ catalyst (Fig. 5). Hence we suggested that the 50 mol% $BaBr_2/Ho_2O_3$ catalyst had degraded in the ODE reaction due to the loss of bromine.

### *Defect Formation and $O_2$ Activation*

Based on the results in Fig. 1 and Table 1, one can realize that after 40 h of ODE reactions and a loss of 34% of its original Br content (Table 6), a 50 mol% $BaBr_2/Ho_2O_3$ catalyst still performed better than a $Ho_2O_3$ catalyst. It is

apparent that the $Br^-$ ions in the $BaBr_2/Ho_2O_3$ catalyst were playing a role in promoting $Ho_2O_3$. Detailed XRD investigations of the $BaBr_2/Ho_2O_3$ catalysts revealed that the addition of $BaBr_2$ to $Ho_2O_3$ could result in the enlargement of the $Ho_2O_3$ lattice. Such change in lattice structure of cubic $Ho_2O_3$ was a result of ionic substitutions. The size of $Ba^{2+}$ ion (radius, 1.43 Å (26)) is larger than that of $Ho^{3+}$ ion (radius, 0.894 Å (26)). If certain amount of $Ba^{2+}$ ions entered into the lattice of $Ho_2O_3$, due to the facts that $Ba^{2+}$ is larger in size and induces smaller Coulombic force, the occupancy of $Ho_2O_3$ lattice points by $Ba^{2+}$ ions would cause the $Ho_2O_3$ lattice to expand. Along with the infiltration of the $Ba^{2+}$ ions, certain amount of $O^{2-}$ ions inside the $Ho_2O_3$ lattice could be replaced by the incoming $Br^-$ ions, and the $Ho_2O_3$ lattice would enlarge even more. If this happened, an electron would be trapped next to the $Br^-$ ion to maintain electric neutrality, and oxygen activation could be enhanced as a result. We have studied the 20 mol% $SrF_2$/SmOF and $BaF_2$/SmOF catalysts previously, and found that ionic substitutions of similar nature would induce the formation of trapped electrons, enhancing oxygen activation as a result (27, 28). We have also detected EPR signals of trapped electrons and $O_2^-$ ions over the 5 mol% $Y_2O_3/BaF_2$ catalyst (24). Osada *et al.* (29) studied the $Y_2O_3$/CaO catalysts for the OCM reaction and reported the formation of $Y_2O_3$-CaO solid solution and lattice distortions of $Y_2O_3$. They concluded that the increase in $C_{2+}$ selectivity at 600 and 700°C with the addition of $Y_2O_3$ to CaO was due to the formation of the solid solution of $Y_2O_3$-CaO and the presence of interstitial oxygen ions $O_2^-$. The results in Tables 1 and 2 show that the oxygen and $C_2H_6$ conversions over the 50 mol% $BaBr_2/Ho_2O_3$ catalyst were higher than those over the pure $Ho_2O_3$ sample. We suggest that the increase in $C_2H_6$ conversion could be related to the enhancement in oxygen activation. For a 90 mol% $BaBr_2/Ho_2O_3$ catalyst, the $O_2$ and $C_2H_6$ conversions were, respectively, 64 and 41%, considerably lower than those of undoped $Ho_2O_3$. From the $O_2$-TPD (Fig. 4), and $O_2$-pulse (Table 7) results, one can realise that the amount of oxygen in a 90 mol% $BaBr_2/Ho_2O_3$ catalyst was much lower than that in a 50 mol% $BaBr_2/Ho_2O_3$ or $Ho_2O_3$ catalyst. With the reduction in the amount of activated oxygen, the conversion of $C_2H_6$ over the catalyst was limited.

*Modification of Surface Basicity by $Br^-$ Ions*

Lunsford *et al.* (1, 2) studied the ODE reaction over the Li-Mg-Cl catalysts, and pointed out that surface basicity was influencing the activities of the catalysts. If the surface basicity of a catalyst was very large, strong $CO_2$ adsorption would occur on the catalyst surface, resulting in low catalytic activity. For a Li-Mg-Cl catalyst with $Cl/Li \geq 0.9$, they observed that the $CO_2$ formed during the ODE reaction did not poison the catalyst, and hence the catalytic activity remained high (1, 2). Similar phenomenon was observed in our studies. For the 50 mol% $BaBr_2/Ho_2O_3$ catalyst, $CO_2$-TPD result indicated that a large amount of $CO_2$ could desorb below 640°C, implying that the catalyst was not strongly basic. Due to the desorption of $CO_2$ at the reaction temperature (ca 640°C) adopted for the ODE reaction, there were active basic sites available for the reaction.

The main carbon-containing products of the ODE reaction are $C_2H_4$, CO, and $CO_2$. There are two ways of producing CO and $CO_2$. They are the deep oxidations of $C_2H_6$ and $C_2H_4$. By using $^{13}C$-labeled $C_2H_4$ and $C_2H_6$, Lunsford *et al.* (30) found that at or above 650°C, $C_2H_4$ was the major source of $CO_x$ formation. This suggests that if the oxidation of $C_2H_4$ can be inhibited, $C_2H_4$ selectivity could improve. From the results of $C_2H_4$ and $C_2H_6$ oxidation in Table 4, one can observe that the catalyst which gave lower $C_2H_4$ conversion in the $C_2H_4$ oxidation reaction would give higher $C_2H_4$ selectivity and $C_2H_6$ conversion in the $C_2H_6$ oxidation reaction. These results advocate that high $C_2H_4$ selectivity in ODE reaction over $BaBr_2/Ho_2O_3$ catalysts could be obtained by suppressing the deep oxidation of $C_2H_4$.

From Table 3, it could be seen that with the increase of space velocity, the $C_2H_4$ selectivity increased. This suggested that $C_2H_4$ deep oxidation could be avoided by shortening the contact time of $C_2H_4$ on the catalyst surface. From the $CO_2$-TPD results, we know that at the adopted reaction temperatures, $CO_2$ could desorb from the 50 mol% $BaBr_2/Ho_2O_3$ catalyst, implying that certain amount of medium-to-strong basic sites were still available on the catalyst surface at ODE reaction conditions. Since $C_2H_4$ molecules normally adsorb on acidic sites, the existence of basic sites would mean poor $C_2H_4$ adsorption; i.e., the contact time of $C_2H_4$ on the catalyst surface became shortened. As a result, the chance of $C_2H_4$ being oxidised was reduced and the selectivity of $C_2H_4$ was enhanced.

*Effects of Limited Oxygen Source*

At near 100% oxygen conversion, the increase of $C_2H_4$ selectivity would mean higher $C_2H_6$ conversion. The following chemical equations show the oxidation of ethane:

Selective oxidation,

$$C_2H_6 + 1/2O_2 \rightarrow C_2H_4 + H_2O; \quad [1]$$

Deep oxidation,

$$C_2H_6 + 5/2O_2 \rightarrow 2CO + 3H_2O \quad [2]$$

$$C_2H_6 + 7/2O_2 \rightarrow 2CO_2 + 3H_2O. \quad [3]$$

One can see that the deep oxidation reactions, [2] and [3], require more oxygen than the selective oxidation reaction, [1]. At near 100% oxygen conversion, if reactions [2] and [3] were suppressed, $C_2H_6$ conversion would increase because the oxygen channelled to the selective oxidation reaction

would convert more $C_2H_6$ molecules in reaction [1] than in reactions [2] and [3].

Burch *et al.* (14) have studied some chloride-promoted oxide catalysts and suggested that the presence of $Cl^-$ ions on the catalyst surface can eliminate the sites for total oxidation and create new active sites for the dehydrogenation of $C_2H_6$ to $C_2H_4$, causing $C_2H_4$ selectivity to be enhanced as a result. Since the formation of CO or $CO_2$ from $C_2H_6$ requires much more oxygen than the formation of $C_2H_4$, we suggest that small clusters of less than five oxygen atoms would favour the selective oxidation reaction. For example, if one $C_2H_6$ molecule is oxidised to CO and $H_2O$, an oxygen cluster containing at least five oxygen atoms is needed. If the cluster contains less than five oxygen atoms, the $C_2H_6$ molecule cannot be fully oxidised to CO and $H_2O$ but would be oxidised selectively to $C_2H_4$. It is possible that the presence of $Br^-$ ions could hinder the formation of large oxygen clusters. This would lead to the suppression of $CO_x$ formation and, hence, the enhancement of $C_2H_4$ selectivity.

For the 50 mol% $BaO/Ho_2O_3$ catalyst, XRD results indicated that there were ionic substitutions between $Ba^{2+}$ and $Ho^{3+}$, and defects capable of activating oxygen were generated. The TPR, $O_2$-TPD, and $O_2$-pulse results showed that the amount of adsorbed oxygen in this sample was large. The results of catalytic performance showed that the conversion of oxygen in the ODE reaction over this catalyst was very high, but the $C_2H_6$ conversion and $C_2H_4$ selectivity were relatively low (Table 1). From the $CO_2$-TPD results, we observed that below 700°C, only a small amount of $CO_2$ could desorb from the catalyst within the temperature range suitable for the ODE reaction, and a large amount of $CO_2$ was desorbed above 750°C. This means that the surface basicity of 50 mol% $BaO/Ho_2O_3$ was large and the catalyst was easily poisoned by $CO_2$ and could not function catalytically below 660°C. For the ODE reaction, sites with medium-to-strong basicity are most suitable. Taking the desorption of $CO_2$ between 400 and 700°C as an indication of the number of active sites with such strength of basicity, the actual strength of surface basicity of the catalysts followed the sequence of 50 mol% $BaBr_2/Ho_2O_3 > Ho_2O_3 >$ aged 50 mol% $BaO/Ho_2O_3$. This order is in accord with the fact that the 50 mol% $BaBr_2/Ho_2O_3$ catalyst showed the highest $C_2H_4$ selectivity while the aged 50 mol% $BaO/Ho_2O_3$ catalyst the lowest (Tables 1 and 2). Due to the complete absence of suitable basic sites on the degraded $BaO/Ho_2O_3$ catalyst, adsorption and reaction of $C_2H_4$ were the most intense and both $C_2H_6$ conversion and $C_2H_4$ selectivity were the worst among the three catalysts. At the conditions of near 100% $O_2$ conversion, the decrease in $C_2H_4$ selectivity would mean lower $C_2H_6$ conversion as more oxygen was consumed in the deep oxidation reactions. Hence, for the aged 50 mol% $BaO/Ho_2O_3$ catalyst, although the oxygen conversion was high, the $C_2H_6$ conversion was low.

## CONCLUSION

Moderate catalytic activity and $C_2H_4$ selectivity in the ODE reaction were observed over the undoped $Ho_2O_3$ catalyst. The addition of BaO could not improve the catalytic performance of $Ho_2O_3$ due to $BaCO_3$ formation. The performance of $Ho_2O_3$, however, could be improved significantly by the addition of 50 mol% of $BaBr_2$. The promotion effects of $BaBr_2$ could be due to several reasons. First, ionic substitutions between the $BaBr_2$ and $Ho_2O_3$ phases could generate defects suitable for oxygen activation. Second, the presence of $Br^-$ ions could modify the surface basicity of the catalyst, leading to the suppression of $C_2H_4$ deep oxidation. Third, it is possible that the presence of $Br^-$ on the catalyst would favour the formation of small oxygen clusters suitable for $C_2H_4$ formation. At near 100% oxygen conversion, with the increase in $C_2H_4$ selectivity, $C_2H_6$ conversion increased because, compared to the deep oxidation reactions, a less amount of oxygen was required to convert $C_2H_6$ to $C_2H_4$ in the selective oxidation of $C_2H_6$. However, with the increase in reaction time, there was continuous leaching of bromine, and the 50 mol% $BaBr_2/Ho_2O_3$ catalyst degenerated to a somewhat aged $BaO/Ho_2O_3$ catalyst.

## ACKNOWLEDGMENTS

The project was supported by the Hong Kong Research Grants Council, UGC (HKBU2050/97P).

## REFERENCES

1. Wang, D., Rosynek, M. P., and Lunsford, J. H., *J. Catal.* **151**, 155 (1995).
2. Conway, S. J., and Lunsford, J. H., *J. Catal.* **131**, 513 (1991).
3. Sugiyama, S., Sogabe, K., Miyamoto, T., Hayashi, H., and Moffat, J. B., *Catal. Lett.* **42**, 127 (1996).
4. Kennedy, E. M., and Cant, N. W., *Appl. Catal.* **75**, 321 (1991).
5. Erdöhelyi, A., Máté, F., and Solymosi, F., *J. Catal.* **135**, 563 (1992).
6. Erdöhelyi, A., and Solymosi, F., *J. Catal.* **129**, 497 (1991).
7. Kennedy, E. M., and Cant, N. W., *Appl. Catal.* **87**, 171 (1992).
8. Yi, G., Hayakawa, T., Andersen, A. G., Suzuki, K., Hamakawa, S., York, A. P. E., Shimizu, M., and Takehira, K., *Catal. Lett.* **38**, 189 (1996).
9. Chang, Y. F., Somorjai, G. A., and Heinemann, H., *J. Catal.* **154**, 24 (1995).
10. Au, C. T., Zhou, X. P., and Wan, H. L., *Catal. Lett.* **40**, 101 (1996).
11. Conway, S. J., Wang, D. J., and Lunsford, J. H., *Appl. Catal.* **79**, L1 (1991).
12. Baldwin, T. R., Burch, R., Crabb, E. M., Squire, G. D., and Tsang, S. C., *Appl. Catal.* **56**, 219 (1989).
13. Lunsford, J. K., Hinson, P. G., Rosynek, M. P., Shi, C., Xu, M., and Yang, X., *J. Catal.* **147**, 301 (1994).
14. Burch, R., Crabb, E. M., Squire, G. D., and Tsang, S. C., *Catal. Lett.* **2**, 249 (1989).
15. Burch, R., Squire, G. D., and Tsang, S. C., *Appl. Catal.* **46**, 69 (1989).
16. Otsuka, K., Hatano, M., and Komatsu, T., *Catal. Today* **4**, 409 (1989).
17. Fujimoto, K., Hashimoto, S., Asami, K., Omoto, K., and Tominaga, H., *Appl. Catal.* **50**, 223 (1989).
18. Ahmed, S., and Moffat, J. B., *J. Catal.* **121**, 408 (1990).
19. Au, C. T., He, H., Lai, S. Y., and Ng, C. F., *J. Catal.* **159**, 280 (1996).

20. Au, C. T., Zhang, Y. Q., He, H., Lai, S. Y., and Ng, C. F., *J. Catal.* **167**, 354 (1997).
21. Au, C. T., He, H., Lai, S. Y., and Ng, C. F., *Appl. Catal.* **159**, 133 (1997).
22. Au, C. T., He, H., Lai, S. Y., and Ng, C. F., *J. Catal.* **163**, 399 (1996).
23. Au, C. T., Liu, Y. W., and Ng, C. F., *J. Catal.* **171**, 231 (1997).
24. Au, C. T., Zhou, X. P., Liu, Y. W., Ji, W. J., and Ng, C. F., *J. Catal.* **174**, 153 (1998).
25. Au, C. T., Chen, K. D., and Ng, C. F., to be published.
26. Cotton, F. A., and Wilkinson, G., "Advanced Inorganic Chemistry," 3rd ed., Interscience, New York, 1972.
27. Au, C. T., and Zhou, X. P., *J. Chem. Soc. Faraday Trans.* **93**, 485 (1997).
28. Au, C. T., and Zhou, X. P., *J. Chem. Soc. Faraday Trans.* **92**, 1793 (1996).
29. Osada, Y., Koike, S., Fukushima, T., Ogasawara, S., Shikada, T., and Ikariya, T., *Appl. Catal.* **59**, 59 (1990).
30. Wang, D. J., Rosynek, M. P., and Lunsford, J. H., *J. Phys. Chem.* **98**, 8371 (1994).